Surgical Resection Facilitates the Access of Intravenously Administered Nanoparticles to Brain Vasculature in Mice

Sara Belko
Thomas Jefferson University
Oluwatobi Babayemi
Rice University
Cassandra Baker
The University of Texas Health Science Center at Houston
Martha Fowler
Rice University
Milad Pourbaghi Masouleh
University of Texas Health Science Center at Houston
Kyle T. Householder
Teva Pharmaceutical Industries Ltd
Sarah E Stabenfeldt
Arizona State University
Rachael W Sirianni (rachael.w.sirianni@uth.tmc.edu)
University of Texas Health Science Center at Houston

Research Article

Keywords: neurosurgery, nanoparticle, central nervous system, brain, resection

Posted Date: July 20th, 2021

DOI: https://doi.org/10.21203/rs.3.rs-704464/v1

Abstract

Nanoparticle systems are often used to facilitate drug delivery to the central nervous system (CNS). There are many clinical situations in which CNS tissue might be removed prior to administration of a therapeutic nanoparticle; however, the iatrogenic effects of surgical resection on nanoparticle deposition in the brain remain unknown. We hypothesized that resection would facilitate nanoparticle delivery to peri-resection tissue as a function of timing of nanoparticle administration after removal of tissue. To test this hypothesis polystyrene nanoparticles surface modified with poly(ethylene glycol) (PEG) were administered either immediately, 2 hours, 24 hours, 4 days, or 7 days after resection of murine cortex. Fluorescence microscopy revealed that minimal nanoparticle delivery to brain vasculature was observed in healthy mice, yet significant nanoparticle delivery was observed in mice that received resection. Spatially, nanoparticles were confined to the vascular compartment and did not enter the parenchyma. Nanoparticle delivery was high near the resection boundary and declined with distance into the peri-resection tissue. The highest level of delivery was observed when nanoparticles were administered immediately after resection, and FNPs could be detected in the CNS when nanoparticles were administered up to 24 hours after resection. The diameter of blood vessels that contained nanoparticles was significantly greater than the diameter of blood vessels that did not contain nanoparticles, and larger vessels contained brighter clusters of nanoparticles. These relationships depended on time after resection, suggesting that a dynamic vascular response. These studies highlight important considerations that can be used to develop nanotechnology for neurosurgical applications.

Introduction

The blood brain barrier (BBB) is an evolutionarily conserved network of cells and cellular processes that serves to maintain homeostasis and protect the brain parenchyma from circulating toxins or pathogens [1]. Its regulatory capacity is both complex and redundant, consisting of tight junctions between endothelial cells that lack of fenestrations, which prevents passive diffusion of water-soluble molecules, as well as efflux transporters that actively deplete molecules that would otherwise gain entry through cellular routes [2]. Few systemically administered agents can reach the brain or spinal cord parenchyma. Molecules that possess the biophysical characteristics necessary for BBB passage (i.e., non-polar and low molecular weight) are plagued by poor aqueous solubility and binding to proteins and lipids, which facilitate rapid clearance from circulation [3]. Thus, the BBB has been a major obstacle that prevents effective treatment of central nervous system (CNS) disease.

Encapsulation of small molecules within nanoparticle carriers is one method that can improve drug delivery across the BBB [4]. Nanoparticle systems afford sustained release of their payload and function either by enhancing circulating levels of active agents nonspecifically, which allows greater opportunity for brain-available substances to reach tissues of interest, or through active targeting strategies that aim to redirect tissue- and cellular-level fate of nanoparticle or payload. In some examples, particle systems have been engineered for transcytosis of both the nanoparticle and its cargo across the BBB into the parenchyma [4][5][6]However, even in absence of nanoparticle transcytosis across the BBB, nanoparticles

are capable of enhancing brain delivery of small molecules [7], thus yielding new opportunities to treat CNS disease in preclinical models[8].

The interaction of nanoparticles with vasculature is known to be a key determinant of drug delivery, and disruption of BBB integrity can offer a selective advantage to nanoparticle mediated drug delivery. For example, it is well established that nanoparticles are capable of accumulating in the leaky vasculature that fuels many intracranial tumors [9][10]. We have also specifically studied nanoparticle delivery following traumatic brain injury (TBI) in mice. In models of controlled cortical impact (CCI) and fluid percussion injury (FPI), there is a spatiotemporally defined window following the injury event, during which nanoparticles are capable of not only accumulating at the site of injury but in fact extravasating into the parenchyma [11][12][13]. Improvements in nanoparticle delivery to the CNS have also been observed in a variety of models in which the integrity of the BBB has been disrupted [14][15][16][17]. Thus, timing of nanoparticle delivery following injury is an important aspect of optimizing therapeutic efficacy for systemically administered nanomedicine.

Building off this prior work demonstrating that injury can facilitate nanoparticle delivery to the CNS, we hypothesize that surgical resection is a form of brain injury that may also affect BBB integrity to alter delivery of systemically administered nanoparticles to the CNS. These iatrogenic effects of surgical resection on nanoparticle delivery have not been studied previously. Here, we subjected healthy mice to a mock surgical resection in the cortex, after which fluorescently labeled, polystyrene nanoparticles surface modified with polyethylene glycol (PEG) were administered intravenously at various time points after injury (immediately, 2 hours, 24 hours, 4 days, or 7 days later). One hour following administration of these model nanoparticles, brains were extracted and fluorescence imaging was used to evaluate the spatial distribution of nanoparticles near to and far from the injury site. Our data support the expectation that resection of brain tissue impacts nanoparticle delivery, and that this is spatiotemporally regulated. These results highlight that timing of nanoparticle administration following surgical resection could be an important mediator of delivery to the CNS, which may have implications for therapeutic development of nanomedicine for neurosurgical applications.

Methods

Nanoparticle Preparation and Characterization

FluoSphere™ polystyrene nanoparticles with starting diameter of 100 nm and carboxylate surface functionality were obtained from Thermo Fisher Scientific (Waltham, MA USA). Nanoparticles were surface modified utilizing carbodiimide chemistry. N-hydroxysuccinimide (NHS, Thermo Fisher) and 1-ethyl-3-(3-dimethylaminopropyl) carbodiimide (EDC, Thermo Fisher) enabled covalent attachment of 2kDa methoxy-poly(ethylene glycol)-amine (mPEG-amine, Nanocs, New York, NY) as previously described [18]. Nanoparticles were washed with distilled water using 0.5 ml Amicon-Ultra centrifugation filters (10k MWCO, MilliporeSigma). mPEG-amine (5x molar excess) was added to nanoparticle solutions and allowed to stir for 15 min. NHS (6.5 mg) was dissolved in borate buffer (6mL 200 mM, pH 8) and added

to the nanoparticle solution, followed by EDC (15.4 mg). After 3 hours, the reaction was quenched with excess glycine (100 mM) for 30 min. Modified nanoparticles were dialyzed (100k MWCO) for 24 hours, washed, and collected with Amicon-Ultra centrifugation filters (100k MWCO). The resulting PEGylated FluoSpheres™ (FNPs) were resuspended to a final concentration of 20 mg/ml in 1x PBS for storage at 4°C. Size and zeta potential of FNPs were measured in 1 mM KCl before and after PEGylation using a NanoBrook 90Plus Zeta (Brookhaven Instruments, Holtsville, NY USA).

Tumor Resection

All procedures were completed in accordance with the Barrow Neurological Institute's Institutional Animal Care and Use Committee. Female C57bl/6 mice (6–8 weeks, Harlan Laboratories, Indianapolis, IN USA) were housed on a 12hr light-dark cycle with *ad libitum* access to food. To simulate surgical injury, we developed a mock resection model. Mice were anesthetized with an intraperitoneal injection of ketamine (100 mg/kg) and xylazine (10 mg/kg). Following excision and retraction of the skin, a handheld biopsy punch was used to remove a portion of the skull, and the dura was carefully dissected from the surface of the brain. A glass pipette vacuum apparatus was used to remove healthy brain tissue from the frontal lobe in the right hemisphere to make a 2 millimeter diameter cavity that extended to reach white matter tracts of the hippocampus. A gelatin sponge (Surgifoam®, Ethicon US, LLC) was used to stop the bleeding. The sponge was removed prior to wound closure, and mice were provided ibuprofen in their drinking water for postsurgical analgesia.

Nanoparticle Administration

FNPs were sonicated for fifteen minutes prior to administration. A total FNP volume of 0.2mL was administered intravenously by lateral tail vein injection to 3–4 mice in each group at the following time points: immediately, 2 hours, 24 hours, 4 days, or 7 days after mock resection. Control mice received injections of PBS after mock resection. The NPs were allowed to circulate for 1 hour, after which the mice were perfused with heparinized PBS.

Tissue Collection and Processing

Following perfusion, the brain was isolated by blunt dissection and post-fixed with 4% paraformaldehyde solution for 24 hours, transferred to a 10% sucrose solution for a minimum of 24 hours or until the brain sank, and flash frozen followed by storage at -80°C. A cutting block was used to slice the brain into ~ 2 millimeter segments, which were then cryo-sectioned to a thickness of 20 μm. Three locations were defined for analysis: ipsilateral (surgically resected hemisphere), contralateral (uninjured hemisphere), and control (control hemisphere from mice that did not receive surgical resection). Slices were stained with an anti-CD31 antibody (Abcam, 1:50 dilution), an endothelial cell marker, for 24 hours at 4°C, washed six times in 0.1% Triton-X, incubated with the secondary antibody (Goat anti-rabbit, 1:500 dilution, Abcam), and washed again six times in 1% Triton-X. Slides were counterstained with DAPI (Vector Laboratories, Burlingame, CA) and cover-slipped. Fluorescent confocal microscopy (Zeiss LSM 710) was performed on every 3rd serial section, keeping acquisition settings constant for different samples.

Image Analysis

Image analyses were performed in ImageJ (v1.47, National Institutes of Health). Only linear image adjustments were utilized, and these were applied equivalently to all images collected. Control samples (in which mice received an injection of saline instead of FNPs) were used to determine background autofluorescence, and all images were corrected to remove background by linear subtraction. A custom-designed MATLAB program [19] was used to map pixel intensity as a function of radial distance from the user-defined resection cavity. These data were binned and averaged across images (3–4 per mouse) and mice (3–4 per group) to develop mean concentration profiles as a function of distance. Blood vessel diameter was measured from tissue slices stained with CD31 by utilizing a linear measurement tool. ROI intensity (a relative measurement of FNP concentration) was determined by measuring mean pixel intensity for a given cluster of nanoparticles and dividing by the area of the cluster, yielding AU/μm^2.

Statistical Methods

Data were analyzed in GraphPad Prism (version 9.1, GraphPad Software, Inc., La Jolla CA). Analyses were conducted utilizing one-way or two-way analysis of variance (ANOVA) as appropriate. Tukey's posthoc testing was utilized to account for multiple comparisons. The alpha level was set to 0.05.

Results

Successful surface modification of nanoparticles was confirmed by dynamic light scattering (DLS). Prior to PEGylation, nanoparticles possessed an average hydrodynamic diameter of 116 ± 2.9 nm. As expected, following PEGylation, the diameter of nanoparticles (now referred to as FNPs) increased to 135 ± 27nm. These observations confirm that the nanoparticles were successfully surface-modified with PEG, in accordance with our prior work that utilized the same conjugation strategy [20].

To assess brain delivery, tissue slices obtained from mice that received intravenous injection of FNPs were analyzed by fluorescence microscopy. Minimal to no FNPs were detected in the brains of control mice (data not shown). In mice that received surgical resection, we studied the spatial distribution of FNPs in ipsilateral (the hemisphere that was resected) and contralateral (the hemisphere that was not resected) regions as a function of time of administration after resection. Although FNPs were occasionally detected in the contralateral hemisphere (Fig. 1A), these FNPs signals were rare, and their location within the brain showed no patterns of localization. We therefore do not consider this signal to be reliable evidence of parenchymal entry. In contrast, FNPs were reliably detected at very high concentration in peri-resection tissue with reproducible patterns of localization when nanoparticles were delivered immediately, 2 hours, or 24 hours after resection (Fig. 1B). FNPs tended to cluster with a spatial distribution indicating containment within brain capillaries. The highest delivery of FNPs was achieved when FNPs were administered immediately following resection, and delivery of FNPs declined when they were administered 2 or 24 hours after resection. Minimal to no FNPs were detected in the brain when FNPs were administered 4 or 7 days after resection. Either immediately, at 2 hours, or at 24 hours after resection, the highest FNP signal was observed in tissue closest to the resection boundary, with the relative prevalence of FNP positive vessels decreasing as distance increased from the resection

boundary. Quantitative analyses revealed that FNP concentration declined within distance into peri-resection tissue (Fig. 1C). FNPs were reliably detected up to 1,000 μm from the resection edge, with only sporadic signal beyond this distance. Given that no FNPs were detected in the brain when they were administered 4 or 7 days after resection, moving forward, results will be provided for mice that received nanoparticles either immediately, 2 hours, or 24 hours after resection.

When FNPs were detected in peri-resection brain, they almost exclusively colocalized with CD31 + vasculature (Fig. 2). In the rare example of FNPs being detected outside of CD31 + vasculature (not shown), we cannot exclude the possibility of a tissue slicing artifact (e.g., FNPs being dragged from vascular locations into the parenchyma by the slicing blade). These examples were sporadic to non-existent in the tissues analyzed, and so we do not attribute this signal to parenchymal entry of FNPs.

We observed that some CD31 + vessels in the brain contained a high concentration of FNPs, while other CD31 + vessels contained no FNPs. To explore the possibility that vessels containing FNPs possess different features than vessels not containing FNPs, we assessed the relationship between ROI intensity (AU/μm^2), blood vessel diameter (μm), and distance from the resection cavity (μm). In contrast to the spatially averaged concentration profiles shown in Fig. 1, these analyses focus on FNP signal measured within discrete, non-uniform regions of interest: i.e., bright clusters containing a high concentration of FNPs would have a high ROI intensity, while dim clusters containing a low concentration of FNPs would have a low ROI intensity. This analysis yielded several intriguing results. First, we observed that BVD in peri-resection tissue was greater when FNPs were administered either immediately or 2 hours after injury compared to when FNPs were administered 24 hours after injury, and these differences were statistically significant (Fig. 3A). There was no apparent relationship between blood vessel diameter and distance from the resection boundary within the relatively confined regions (up to 2mm from the resection boundary) that we analyzed (Fig. 3B). There were significant differences in vessel properties for capillaries that did or did not contain FNPs (Fig. 4). BVD was lowest in the contralateral (non-resected) hemisphere. BVD in the ipsilateral (resected) hemisphere) depended on whether the capillary contained or did not contain FNPs. Vessels that contained FNPs possessed a greater diameter than vessels with no detectable FNPs.

We observed that the relative brightness of clusters of FNPs was different in differently sized vessels, and this was a function of time of FNP administration, an independent variable that also influences time of tissue collection after resection (i.e., for mice that received FNPs either immediately, 2, or 24 hours after resection, tissues were collected 1, 3, or 25 hours after resection, respectively). When FNPs were administered immediately after resection, ROI intensity was not related to blood vessel diameter, with many very intense signals observed in relatively small vessels. In contrast, when FNPs were administered 2 or 24 hours after resection, larger vessels contained brighter FNP clusters with a higher ROI intensity (Fig. 5). These data were robust and repeatable, suggesting that a dynamic injury response induces distinct nanoparticle-vessel interactions. The causality of this relationship could not be determined here; either, the injury response influences BVD such that larger vessels are enriched in highly clustered FNPs,

or, the presence of the FNPs themselves directly influences BVD (for example, by preventing effective vasoconstriction after injury).

Discussion

The BBB is an evolutionarily conserved network of endothelial cells that prevents nearly all circulating molecules from reaching the CNS at therapeutically relevant concentrations [2]. Encapsulation of drugs within biocompatible nanoparticles is one method by which their delivery to the CNS can be improved. These improvements are typically achieved via non-specific mechanisms; for example, nanoparticle encapsulation can enhance circulation time and improve local bioavailability of small, lipophilic agents that passively diffuse from the nanoparticle across the BBB [3]. Although large nanoparticles in unmodified form do not circumvent an intact BBB [11], there is evidence that an injured (or diseased) BBB can facilitate nanoparticle accumulation along the vascular endothelium or within the parenchyma of the brain and spinal cord [13] to enable better drug delivery [21]. Importantly, prior work demonstrates that the extent of nanoparticle accumulation depends on the time of their administration after injury to the CNS [12].

Because surgical resection is a form of brain injury, we aimed to characterize how timing of nanoparticle administration after surgical resection impacts CNS delivery of intravenously administered nanoparticles. We hypothesized that nanoparticle delivery to the CNS would be enhanced following mock surgical resection in mice. To test this hypothesis, mice were subjected to mock surgical resection, in which a small volume of brain tissue was vacuum pipetted from the cortex of a single hemisphere. Nanoparticles were administered intravenously at various time points after resection, and their distribution in the brain was studied with fluorescence microscopy both qualitatively and quantitatively.

Our model system utilized solid, fluorescent, non-degradable polystyrene nanoparticles that possess an average hydrodynamic diameter of ~ 135nm following surface modification with PEG. These nanoparticles were selected for several reasons. First, this size is appropriate for engineering long-circulating nanoparticles to avoid clearance by the reticulo-endothelial system (RES) [22]. This average diameter is also within a typical size range for nanoparticle systems that have been designed for CNS drug delivery [23]. Second, we selected a nondegradable nanoparticle with fixed fluorescence signal to ensure that these measurements reflect delivery of an intact nanoparticle versus measurement of a non-covalently linked payload, lost label, or nanoparticle degradation byproduct [24][25]. Lastly, nanoparticles were PEGylated to reduce protein absorption on the surface of the nanoparticle, which is a field standard technique that confers benefits in terms of nanoparticle circulation and cellular interaction [26][27]. These FNP nanoparticles are thus considered a somewhat generic rather than specific example of nanomedicine, which improves the chance that what was observed here could have general relevance to other types of solid nanoparticle systems that have been engineered for CNS drug delivery.

In this work, fluorescence microscopy analyses demonstrated that intravenously administered FNPs are not detected in uncompromised tissues, either in the brains of healthy mice that did not receive surgical

resection, or in the hemisphere that is contralateral to surgical resection. These data confirm prior reports that ~ 100nm nanoparticles do not bypass the BBB in un-modified form [7][28]. In contrast to the lack of CNS delivery observed for an uncompromised BBB, FNPs preferentially accumulated within blood vessels near to resected tissue, with the highest concentration of FNPs observed directly adjacent to the resection cavity and FNP concentration declining with distance from the resection cavity. Because FNPs were almost always associated with blood vessels, were reliably detected at distances far from the resection border (up to 1000μm), and are of relatively large diameter that prevents effective movement through the brain interstitium [29], this concentration gradient is unlikely to represent diffusion of nanoparticle through the parenchyma and must involve a physiological, likely hematogenous or cellular (paracrine), process. It is unlikely that the source of FNP delivery originates from a systemic signal via the hematogenous pathway, given that changes in vessel diameter and nanoparticle delivery were restricted to the injured hemisphere. However, FNP delivery extended well beyond the immediate injury zone. The most likely explanation for the FNP concentration gradient would involve local release and diffusion of a soluble signaling factor from the injury zone into peri-resection tissue, leading to the most significant BBB alterations near to the injury site that then decline with distance.

We observed that the extent of FNP accumulation depended on timing of nanoparticle administration following resection, which confirms prior reports of temporally regulated injury responses. Nanoparticle delivery to a disrupted BBB has been studied in a variety of injury contexts, including traumatic brain injury [11][30], spinal cord injury [16][31][32][33][34][35][36], neuroinflammation [37], oncology [38][14][39], stroke [40][41], cerebral hemorrhage [42][43], and neurodegeneration [15][17][44]. CNS injury can be either acute or chronic, involving both physical damage to the cells that directly disrupts BBB integrity, as well as secondary injury responses that include inflammation and immune cell infiltration and activation [45]. This secondary injury response can further prolong or enhance CNS damage [46][47][48][49][50][51], which is why we opted to examine both acute and chronic administration time points. In prior work, we specifically studied nanoparticle delivery to the brain in controlled cortical impact (CCI, representing focal injury) and fluid percussion injury (FPI, representing diffuse injury) murine models of TBI. These studies utilized similar fluorescent, polystyrene nanoparticles of varying size (20, 40, 100, and 500nm) that were then PEGylated. Although intravenously administered nanoparticles do not reach the parenchyma in the uninjured hemisphere, we have shown in multiple reports that nanoparticles accumulate in the injury zone and injury penumbra as a function of nanoparticle size and time of administration after injury [11] [12] [13]. Qualitatively, the extent of nanoparticle delivery to the parenchyma decreased with distance from the injury site, a spatial pattern of delivery that is similar to our findings here. In the CCI model, nanoparticle accumulation was highest when nanoparticles were administered 1h after injury compared to later times (up to 24h) after injury [11][12]; sex-dependent differences in the timing of this window for delivery were also observed [13]. In contrast, in the FPI model, nanoparticle accumulation peaked when nanoparticles were administered 3h after injury, compared to either 1 hr or later times (up to 24h) [12]. In either model, nanoparticle accumulation was closely related to horseradish peroxidase extravasation, demonstrating a mechanistic correlation between extent of BBB disruption and extent of nanoparticle accumulation in TBI [12]. These published studies support the notion that different injury paradigms could produce distinct

temporal and spatial evolution of BBB breakdown, yielding distinct nanoparticle deposition profiles. Our current data are consistent with this prior work, demonstrating that surgical injury also provides a temporally defined window of opportunity for enhanced nanoparticle delivery to the CNS. However, in the prior TBI work, nanoparticles were distributed well beyond vasculature to reach the parenchyma, whereas in this current work, nanoparticle delivery was confined to the vascular compartment. Additionally, in the TBI studies, the window was prolonged and/or characterized by a secondary peak in male mice, enabling nanoparticle deposition in the parenchyma up to 3 days after injury [13]. In contrast to this prior work in TBI, we observed a relatively short window of opportunity with no evidence for prolonged or secondary opening at the later time points we assessed (24 hours, 4 days, or 7 days after injury). Given that our studies utilized nearly identical model nanoparticles, the contrast between these two studies highlights the complexity of brain injury responses.

The physiology of surgical brain injury is poorly understood [52]. Surgical brain injury occurs as a result of, but not limited to, physical processes that include resection, incision, retraction or thermal damage. The main consequence of such iatrogenic damage is irreversible tissue loss. This loss can also materialize as tumor decompression, which is standard of care for treatment of malignant brain tumors; however, our understanding of how iatrogenic injury impacts vasculature is incomplete. It is known that tumor resection results in impaired regulation of cerebral blood flow [53]. Moreover, rodent models mimicking surgical brain injury suggest that the injury disrupts the BBB, causes neuronal death, and results in brain edema [54]. This pathophysiology is observed in routine surgical settings. BBB dysfunction and corresponding tissue responses thus play a pivotal role in surgical brain injury [55]. It has also been reported that resection of brain tissue may cause significant reorganization of brain structures, this damage is not immediately reversible, and the extent of reorganization is dependent on the location within the brain that resection occurred [56]. In the current work, we focused on a model of resection of the cortex of mice. It is possible that the iatrogenic effect of resection on nanoparticle deposition will depend on brain region, but this remains the subject of future work.

There are several limitations to our current study. Vessels comprising the BBB were identified here through antibody staining for CD31, which is a general vascular stain that effectively labels endothelial cells. All CD31 + signal was observed in cellular formations with a characteristic capillary shape, which further supports that the CD31 + signal represents BBB cells. Our analyses focused on phenotypic changes to the major features of the BBB in an observational context, and it will be the subject of future work to determine which molecular mechanisms underly these differences. Whether the relationships observed here are due to unidirectional (vessel to nanoparticle) or bidirectional (involving both nanoparticle effects on blood vessels as well as as vessel effects on nanoparticles) remains unclear, although it is known that some solid nanoparticles can induce distinct inflammatory responses from endothelial cells[57]. The vessel microenvironment is complex, and tissue engineering approaches may be particularly useful for developing a better understanding of how features such as hemodynamic stress, biomechanical stimulation, or immune responses alter endothelial cell and vessel interactions with nanoparticles[58, 59]. Our results are also specific to the solid, ~ 100nm model nanoparticles utilized in

this study. Whether the relationships observed here extend to other classes of nanomedicine remains to be determined.

We focused on studying the iatrogenic effect of surgical resection on nanoparticle delivery as an example of brain injury. CNS tissues can be removed for a variety of reasons, including biopsy or treatment of a tumor, epilepsy, infection, arteriovenous malformation, or vascular injury resulting from CNS trauma such as stroke or intracerebral hemorrhage. In some instances, resection could involve removal of diseased tissue, in which vascular aberrations are already present (e.g., the poorly formed neovasculature of a rapidly growing tumor). In other instances, resection or related forms of surgical brain injury could occur for tissue that would otherwise possess an intact BBB. This may occur in a clinical setting (e.g., removal of epileptic tissue, or incidental damage that occurs when the brain must be surgically accessed for biopsy or implantation of a catheter), but it is also significant for preclinical models. In preclinical models, the brain is often surgically accessed to induce disease – for example, to implant a tumor, or to infuse a substance that will generate disease-mimicking pathophysiology. It has been shown in published work that these surgical procedures can disrupt the BBB [60]. Our data show that nanoparticle delivery to the CNS is enhanced following surgical resection of tissue in absence of preexisting vascular malformation or damage. These results may have implications for preclinical models in which nanoparticle delivery seems to be demonstrated but in fact could be an artifact of BBB disruption from the surgical procedure. Whether different forms of surgical injury or the combination of surgical injury with other kinds of vascular damage might further alter nanoparticle deposition profiles will be the subject of future studies. Taken in sum, this work is the first to directly address nanoparticle deposition in the brain following iatrogenic injury and raises significant considerations for the development of nanomedicine to treat CNS disease after surgical resection.

Conclusions

Intravenously administered FNPs are not detected in the brains of healthy mice but are readily observed in the brain vasculature of mice that have received mock surgical resection. Our observations support the over-arching hypothesis that iatrogenic surgical brain injury facilitates nanoparticle access to the brain via interaction with vasculature. Specifically, the extent of delivery is spatiotemporally regulated following injury, which is consistent with observations regarding nanoparticle deposition in other preclinical injury models. The data presented here suggest that surgery itself is an important confounder for interpretation of preclinical nanoparticle delivery studies as well as a key variable that might influence therapeutic development for translation of nanomedicine into the clinic.

Declarations

ACKNOWLEDGMENTS

The authors gratefully acknowledge support for this work provided by the National Institutes of Health (R21NS107985, R01NS111292, R01HD099543, and R01NS116657), the Barrow Neurological Foundation,

and Arizona State University. We also acknowledge the database http://www.citeblackauthors.com, which enabled us to contribute to equitable citation practices in academia.

Funding

Funding for this work was provided by the National Institutes of Health (R21NS107985, R01NS111292, R01HD099543, and R01NS116657), the Barrow Neurological Foundation, and Arizona State University.

Conflicts of interest / competing interests

The authors declare no conflicts of interest that are related to the subject of this work.

Per request by the journal on submission, RWS discloses the following relationships. None of these disclosures are expected to yield a conflict of interest or perceived conflict of interest for this work:

1. Employment: UTHealth

2. Consultancies in the last 3 years: Ian's Friends Foundation, Health Advances, Exicure, Inc., Zulia Biotech

3. Honoraria in the last 3 years: Loyola University, Neurovations Education

4. Stock ownership/ options other than mutual funds: none

5. Expert testimony in the last 3 years: none

6. Grants received in the last 3 years: National Institutes of Health (various), Ian's Friends Foundation, the Morgan Adams Foundation, subcontract on the Matthew Larson Foundation

7. Grants pending: none

8. Patents received: US10745478B2, US20200054562A1

9. Patents pending: PCT/WO2018232366A1, PCT/US202024627

10. Royalties: none

11. Other relationships: none

Availability of data and material

All data and pilot quantities of materials used for this work will be made available to any researcher upon request

Code availability

The Matlab code utilized for this work is already published and freely available

Authors' contributions

SB helped design the experiments, conducted the experiments, analyzed the data, and drafted the manuscript. OB, CB, MF, and MPM analyzed the data, interpreted the data, and wrote major sections of text. KTH designed the experiments, assisted in conducting the experiments, and edited the manuscript. SS interpreted the data and edited the manuscript. RWS designed the experiments, analyzed the data, interpreted the data, wrote major sections of text, and was responsible for final drafting and submission of the manuscript.

Ethics approval

The animal studies were conducted at the Barrow Neurological Institute, which AAALAAC accredited and conducts animal work under the supervision of the Institutional Animal Care and Use Committee (IACUC). The protocol number approved for this work is 429.

Consent to participate

Not applicable

Consent to publish

All authors have edited the manuscript, seen the final version of the manuscript, and agreed to submit the manuscript for publication

ETHICAL STANDARDS

The authors declare that all experiments described in this work comply with current laws in the United States of America, which is the country in which all work was performed.

ANIMAL STUDIES

All institutional and national guidelines for the care and use of laboratory animals were followed

References

1. Blanchette M, Daneman R. Formation and maintenance of the BBB. Mechanisms of Development. 2015;138.

2. Pardridge WM. Blood–brain barrier delivery. Drug Discovery Today. 2007;12.

3. Barbu E, Molnàr É, Tsibouklis J, Górecki DC. The potential for nanoparticle-based drug delivery to the brain: overcoming the blood–brain barrier. Expert Opinion on Drug Delivery. 2009;6.

4. Ahn SI, Sei YJ, Park H-J, Kim J, Ryu Y, Choi JJ, et al. Microengineered human blood–brain barrier platform for understanding nanoparticle transport mechanisms. Nature Communications. 2020;11.

5. Ragnaill MN, Brown M, Ye D, Bramini M, Callanan S, Lynch I, et al. Internal benchmarking of a human blood–brain barrier cell model for screening of nanoparticle uptake and transcytosis. European Journal of Pharmaceutics and Biopharmaceutics. 2011;77.

6. B C, JS L, AA A-B. Vectors for Glioblastoma Gene Therapy: Viral & Non-Viral Delivery Strategies. Nanomaterials (Basel, Switzerland) [Internet]. Nanomaterials (Basel); 2019 [cited 2021 Jul 8];9. Available from: https://pubmed.ncbi.nlm.nih.gov/30654536/

7. Cook RL, Householder KT, Chung EP, Prakapenka A v., DiPerna DM, Sirianni RW. A critical evaluation of drug delivery from ligand modified nanoparticles: Confounding small molecule distribution and efficacy in the central nervous system. Journal of Controlled Release. 2015;220.

8. Ceña V, Játiva P. Nanoparticle crossing of blood–brain barrier: a road to new therapeutic approaches to central nervous system diseases. https://doi.org/102217/nnm-2018-0139 [Internet]. Future Medicine Ltd London, UK ; 2018 [cited 2021 Jul 8];13:1513–6. Available from: https://www.futuremedicine.com/doi/abs/10.2217/nnm-2018-0139

9. Fang J, Nakamura H, Maeda H. The EPR effect: Unique features of tumor blood vessels for drug delivery, factors involved, and limitations and augmentation of the effect. Advanced Drug Delivery Reviews. 2011;63.

10. Houston ZH, Bunt J, Chen K-S, Puttick S, Howard CB, Fletcher NL, et al. Understanding the Uptake of Nanomedicines at Different Stages of Brain Cancer Using a Modular Nanocarrier Platform and Precision Bispecific Antibodies. ACS Central Science. 2020;6.

11. Bharadwaj VN, Lifshitz J, Adelson PD, Kodibagkar VD, Stabenfeldt SE. Temporal assessment of nanoparticle accumulation after experimental brain injury: Effect of particle size. Scientific Reports. 2016;6.

12. Bharadwaj VN, Rowe RK, Harrison J, Wu C, Anderson TR, Lifshitz J, et al. Blood–brainbarrier disruption dictates nanoparticle accumulation following experimental brain injury. Nanomedicine: Nanotechnology, Biology and Medicine. 2018;14.

13. Bharadwaj VN, Copeland C, Mathew E, Newbern J, Anderson TR, Lifshitz J, et al. Sex-Dependent Macromolecule and Nanoparticle Delivery in Experimental Brain Injury. Tissue Engineering Part A. 2020;26.

14. Gregory J v., Kadiyala P, Doherty R, Cadena M, Habeel S, Ruoslahti E, et al. Systemic brain tumor delivery of synthetic protein nanoparticles for glioblastoma therapy. Nature Communications. 2020;11.

15. Masoudi Asil S, Ahlawat J, Guillama Barroso G, Narayan M. Nanomaterial based drug delivery systems for the treatment of neurodegenerative diseases. Biomaterials Science. 2020;8.

16. Gao Y, Vijayaraghavalu S, Stees M, Kwon BK, Labhasetwar V. Evaluating accessibility of intravenously administered nanoparticles at the lesion site in rat and pig contusion models of spinal cord injury. Journal of Controlled Release. 2019;302.

17. Zhang Y, Schlachetzki F, Zhang Y-F, Boado RJ, Pardridge WM. Normalization of Striatal Tyrosine Hydroxylase and Reversal of Motor Impairment in Experimental Parkinsonism with Intravenous Nonviral Gene Therapy and a Brain-Specific Promoter. Human Gene Therapy. 2004;15.

18. Nance EA, Woodworth GF, Sailor KA, Shih T-Y, Xu Q, Swaminathan G, et al. A Dense Poly(Ethylene Glycol) Coating Improves Penetration of Large Polymeric Nanoparticles Within Brain Tissue. Science Translational Medicine. 2012;4.

19. Lindner SC, Yu M, Capadona JR, Shoffstall AJ. A graphical user interface to assess the neuroinflammatory response to intracortical microelectrodes. Journal of Neuroscience Methods. 2019;317.

20. Householder KT, Dharmaraj S, Sandberg DI, Wechsler-Reya RJ, Sirianni RW. Fate of nanoparticles in the central nervous system after intrathecal injection in healthy mice. Scientific Reports. 2019;9.

21. Kulkarni SA, Feng S-S. Effects of Particle Size and Surface Modification on Cellular Uptake and Biodistribution of Polymeric Nanoparticles for Drug Delivery. Pharmaceutical Research. 2013;30.

22. Duan X, Li Y. Physicochemical Characteristics of Nanoparticles Affect Circulation, Biodistribution, Cellular Internalization, and Trafficking. Small. 2013;9.

23. Patel T, Zhou J, Piepmeier JM, Saltzman WM. Polymeric nanoparticles for drug delivery to the central nervous system. Advanced Drug Delivery Reviews. 2012;64.

24. Loos C, Syrovets T, Musyanovych A, Mailänder V, Landfester K, Nienhaus GU, et al. Functionalized polystyrene nanoparticles as a platform for studying bio–nano interactions. Beilstein Journal of Nanotechnology. 2014;5.

25. Hu X, Dong X, Lu Y, Qi J, Zhao W, Wu W. Bioimaging of nanoparticles: the crucial role of discriminating nanoparticles from free probes. Drug Discovery Today. 2017;22.

26. Alexis F, Pridgen E, Molnar LK, Farokhzad OC. Factors Affecting the Clearance and Biodistribution of Polymeric Nanoparticles. Molecular Pharmaceutics. 2008;5.

27. Suk JS, Xu Q, Kim N, Hanes J, Ensign LM. PEGylation as a strategy for improving nanoparticle-based drug and gene delivery. Advanced Drug Delivery Reviews. 2016;99.

28. Medina DX, Householder KT, Ceton R, Kovalik T, Heffernan JM, Shankar R v., et al. Optical barcoding of PLGA for multispectral analysis of nanoparticle fate in vivo. Journal of Controlled Release. 2017;253.

29. Syková E, Nicholson C. Diffusion in Brain Extracellular Space. Physiological Reviews [Internet]. 2008 [cited 2021 Jul 5];88. Available from: https://doi.org/10.1152/physrev.00027.2007

30. Li W, Qiu J, Li X-L, Aday S, Zhang J, Conley G, et al. BBB pathophysiology–independent delivery of siRNA in traumatic brain injury. Science Advances. 2021;7.

31. Wang J, Li D, Liang C, Wang C, Zhou X, Ying L, et al. Scar Tissue-Targeting Polymer Micelle for Spinal Cord Injury Treatment. Small [Internet]. 2020 [cited 2021 May 14];16. Available from: https://doi.org/10.1002/smll.201906415

32. Chen B, Zuberi M, Borgens R ben, Cho Y. Affinity for, and localization of, PEG-functionalized silica nanoparticles to sites of damage in an ex vivo spinal cord injury model. Journal of Biological Engineering. 2012;6.

33. Jeffery ND, McBain SC, Dobson J, Chari DM. Uptake of systemically administered magnetic nanoparticles (MNPs) in areas of experimental spinal cord injury (SCI). Journal of Tissue Engineering and Regenerative Medicine [Internet]. 2009 [cited 2021 May 17];3. Available from: https://doi.org/10.1002/term.139

34. Grüner F, Blumendorf F, Schmutzler O, Staufer T, Bradbury M, Wiesner U, et al. Localising functionalised gold-nanoparticles in murine spinal cords by X-ray fluorescence imaging and background-reduction through spatial filtering for human-sized objects. Scientific Reports. 2018;8.

35. Jain S, Pal A, Singh, Nag T, Chattopadhyay, Mathur. Iron oxide nanoparticles and magnetic field exposure promote functional recovery by attenuating free radical-induced damage in rats with spinal cord transection. International Journal of Nanomedicine. 2013;

36. Papastefanaki F, Jakovcevski I, Poulia N, Djogo N, Schulz F, Martinovic T, et al. Intraspinal Delivery of Polyethylene Glycol-coated Gold Nanoparticles Promotes Functional Recovery After Spinal Cord Injury. Molecular Therapy. 2015;23.

37. Calvo P, Gouritin B, Villarroya H, Eclancher F, Giannavola C, Klein C, et al. Quantification and localization of PEGylated polycyanoacrylate nanoparticles in brain and spinal cord during experimental allergic encephalomyelitis in the rat. European Journal of Neuroscience [Internet]. 2002 [cited 2021 May 17];15. Available from: https://doi.org/10.1046/j.1460-9568.2002.01967.x

38. Meyers JD, Doane T, Burda C, Basilion JP. Nanoparticles for imaging and treating brain cancer. Nanomedicine. 2013;8.

39. Medina RJ, Barber CL, Sabatier F, Dignat-George F, Melero-Martin JM, Khosrotehrani K, et al. Endothelial Progenitors: A Consensus Statement on Nomenclature. STEM CELLS Translational Medicine. 2017;6.

40. Bonnard T, Gauberti M, Martinez de Lizarrondo S, Campos F, Vivien D. Recent Advances in Nanomedicine for Ischemic and Hemorrhagic Stroke. Stroke. 2019;50.

41. Wu Q, Yan R, Sun J. Probing the drug delivery strategies in ischemic stroke therapy. Drug Delivery. 2020;27.

42. Choi SW, Kim J. Recent Progress in Autocatalytic Ceria Nanoparticles-Based Translational Research on Brain Diseases. ACS Applied Nano Materials [Internet]. 2020 [cited 2021 May 17];3. Available from: https://doi.org/10.1021/acsanm.9b02243

43. Alkaff SA, Radhakrishnan K, Nedumaran AM, Liao P, Czarny B. Nanocarriers for Stroke Therapy: Advances and Obstacles in Translating Animal Studies. International Journal of Nanomedicine. 2020;Volume 15.

44. Kulkarni P v., Roney CA, Antich PP, Bonte FJ, Raghu A v., Aminabhavi TM. Quinoline-n-butylcyanoacrylate-based nanoparticles for brain targeting for the diagnosis of Alzheimer's disease. Wiley Interdisciplinary Reviews: Nanomedicine and Nanobiotechnology [Internet]. 2010 [cited 2021 May 17];2. Available from: https://doi.org/10.1002/wnan.59

45. McDonald SJ, Sun M, Agoston D v., Shultz SR. The effect of concomitant peripheral injury on traumatic brain injury pathobiology and outcome. Journal of Neuroinflammation. 2016;13.

46. Bruder N, Ravussin P. Recovery from Anesthesia and Postoperative Extubation of Neurosurgical Patients. Journal of Neurosurgical Anesthesiology. 1999;11.

47. Lo W, Bravo T, Jadhav V, Titova E, Zhang JH, Tang J. NADPH oxidase inhibition improves neurological outcomes in surgically-induced brain injury. Neuroscience Letters. 2007;414.

48. Hyong A, Jadhav V, Lee S, Tong W, Rowe J, Zhang JH, et al. Rosiglitazone, a PPAR gamma agonist, attenuates inflammation after surgical brain injury in rodents. Brain Research. 2008;1215.

49. Ayer RE, Jafarian N, Chen W, Applegate RL, Colohan ART, Zhang JH. Preoperative mucosal tolerance to brain antigens and a neuroprotective immune response following surgical brain injury. Journal of Neurosurgery. 2012;116.

50. Lekic T, Rolland W, Manaenko A, Krafft PR, Kamper JE, Suzuki H, et al. Evaluation of the hematoma consequences, neurobehavioral profiles, and histopathology in a rat model of pontine hemorrhage. Journal of Neurosurgery. 2013;118.

51. Sulejczak D, Grieb P, Walski M, Frontczak-Baniewicz M. Apoptotic death of cortical neurons following surgical brain injury. Folia Neuropathologica. 2008;46:213–9.

52. Travis ZD, Sherchan P, Hayes WK, Zhang JH. Surgically-induced brain injury: where are we now? Chinese Neurosurgical Journal. 2019;5.

53. Sharma D, Bithal PK, Dash HH, Chouhan RS, Sookplung P, Vavilala MS. Cerebral Autoregulation and CO2 Reactivity Before and After Elective Supratentorial Tumor Resection. Journal of Neurosurgical Anesthesiology. 2010;22.

54. Jadhav V, Zhang JH. Surgical brain injury: prevention is better than cure. Frontiers in Bioscience [Internet]. 2008 [cited 2021 May 14];Volume. Available from: https://www.bioscience.org/2008/v13/af/2968/fulltext.htm

55. Matchett G, Hahn J, Obenaus A, Zhang J. Surgically induced brain injury in rats: The effect of erythropoietin. Journal of Neuroscience Methods. 2006;158.

56. Lazar M, Alexander A, Badie B, Field A, Thottakara P. White matter reorganization after surgical resection of brain tumors and vascular malformations. American Journal of Neuroradiology. 2006;27:1258–71.

57. Cao Y. The Toxicity of Nanoparticles to Human Endothelial Cells. Advances in Experimental Medicine and Biology [Internet]. Springer, Cham; 2018 [cited 2021 Jul 8];1048:59–69. Available from: https://link.springer.com/chapter/10.1007/978-3-319-72041-8_4

58. J S, A J, H R, T A, E M. Modeled vascular microenvironments: immune-endothelial cell interactions in vitro. Drug delivery and translational research [Internet]. Drug Deliv Transl Res; 2021 [cited 2021 Jul 8]; Available from: https://pubmed.ncbi.nlm.nih.gov/33797034/

59. BD J, JB A. Vascular Endothelial Cell Behavior in Complex Mechanical Microenvironments. ACS biomaterials science & engineering [Internet]. ACS Biomater Sci Eng; 2018 [cited 2021 Jul 8];4:3818–42. Available from: https://pubmed.ncbi.nlm.nih.gov/33429612/

60. Kerklaan JP, Lycklama á Nijeholt GJ, Wiggenraad RGJ, Berghuis B, Postma TJ, Taphoorn MJB. SMART syndrome: a late reversible complication after radiation therapy for brain tumours. Journal of Neurology. 2011;258.

Figures

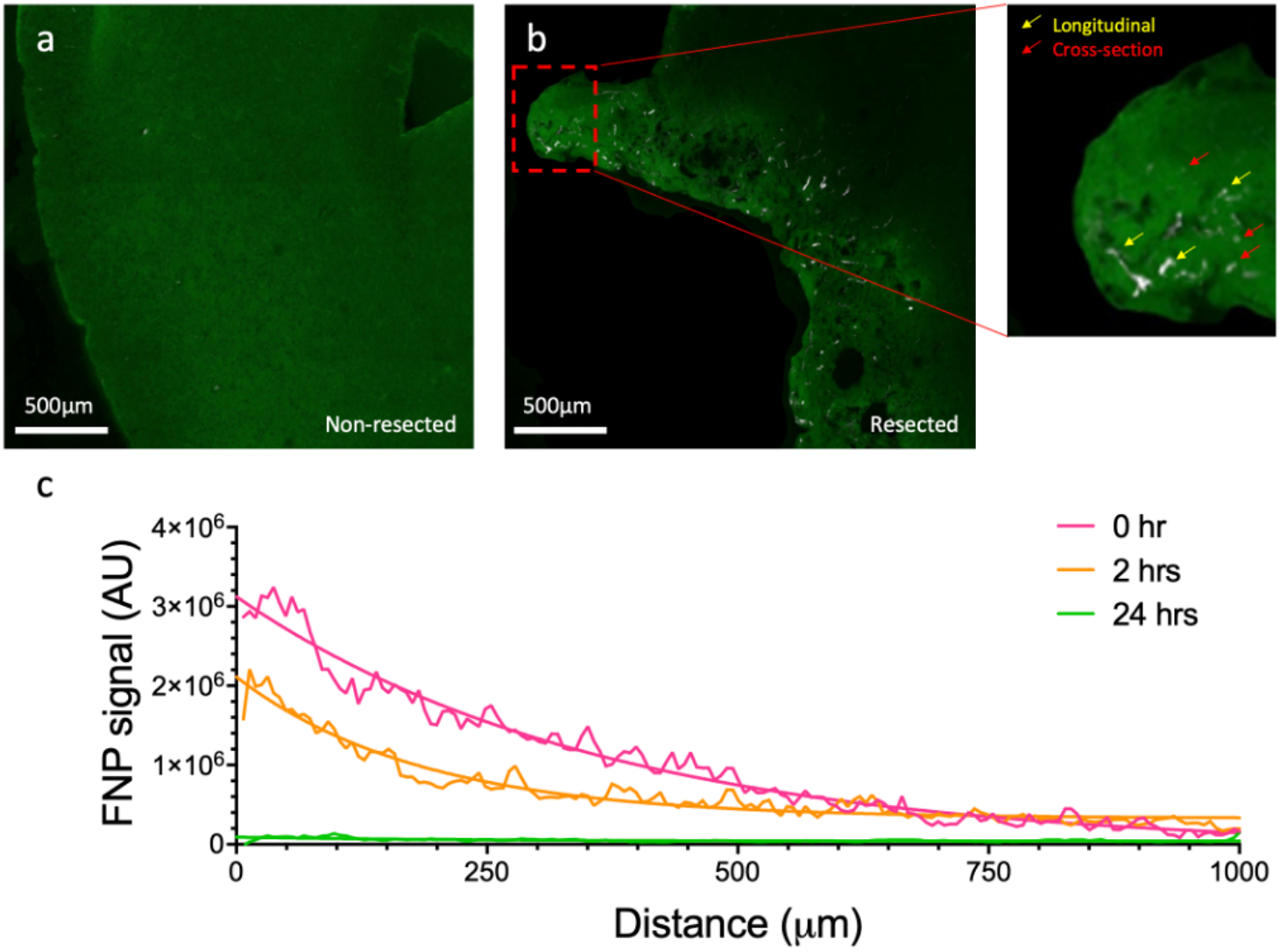

Figure 1

In mice that received surgical resection, we studied the spatial distribution of FNPs in ipsilateral (the hemisphere that was resected) and contralateral (the hemisphere that was not resected) regions as a function of time of administration after resection. Although FNPs were occasionally detected in the contralateral hemisphere

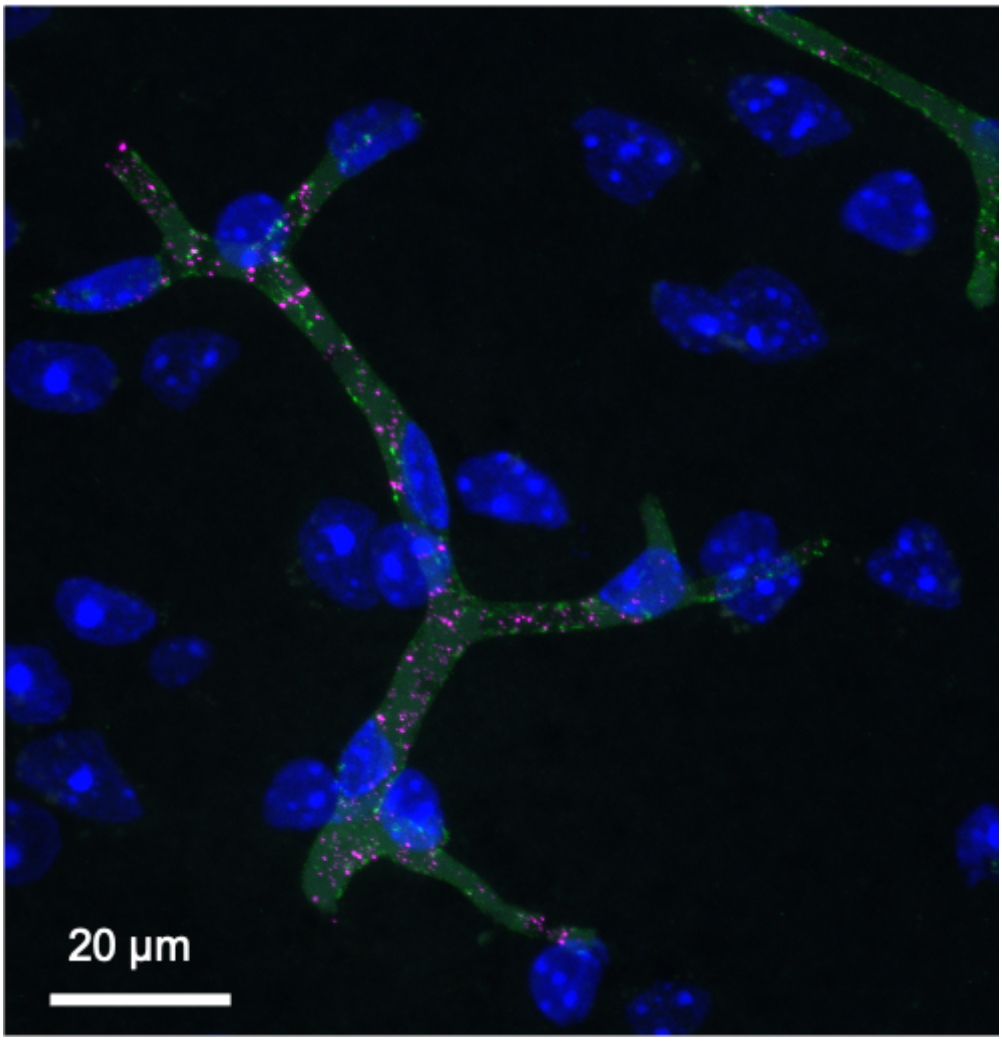

Figure 2

When FNPs were detected in peri-resection brain, they almost exclusively colocalized with CD31+ vasculature (Figure 2).

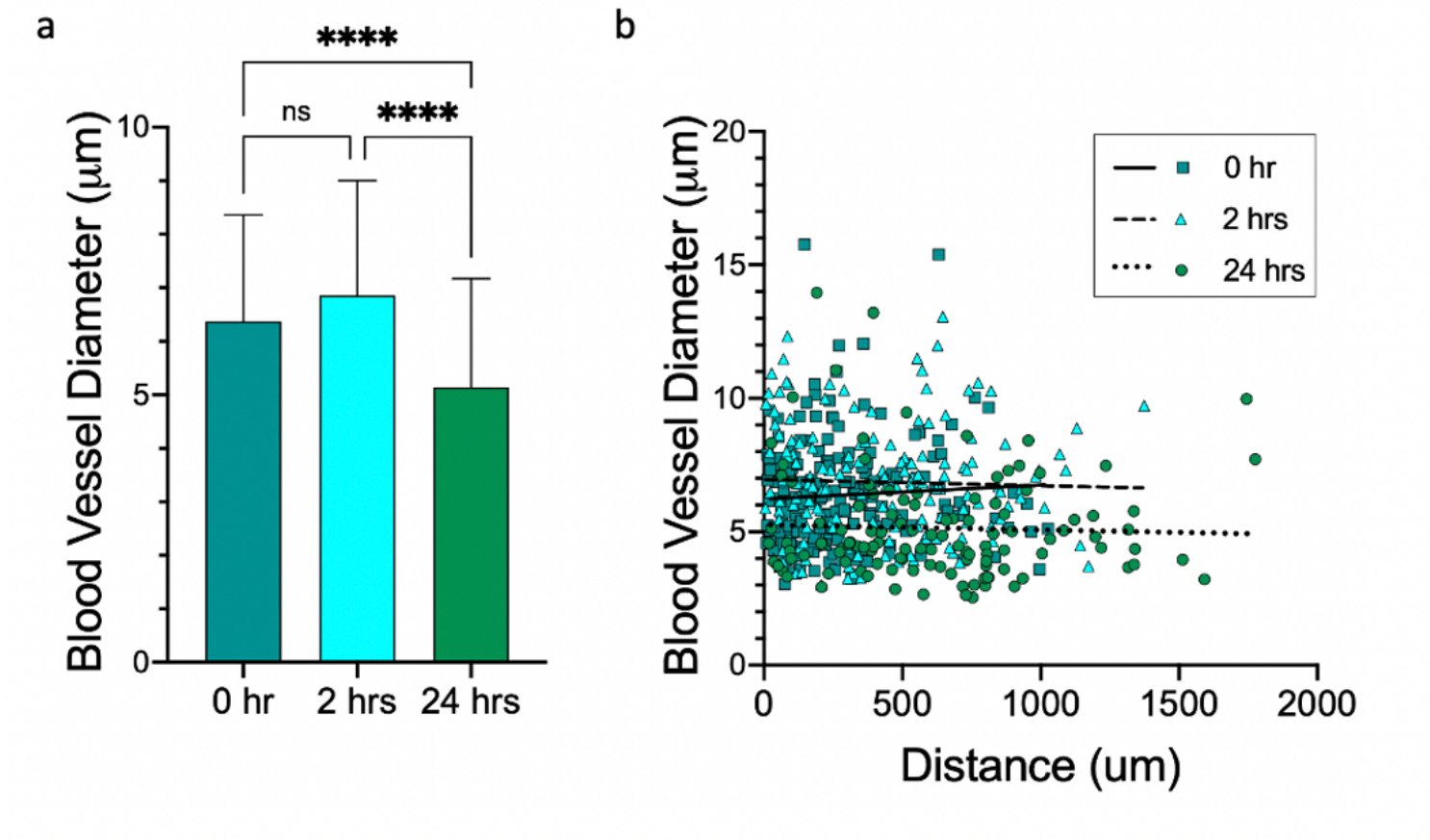

Figure 3

First, we observed that BVD in peri-resection tissue was greater when FNPs were administered either immediately or 2 hours after injury compared to when FNPs were administered 24 hours after injury, and these differences were statistically significant

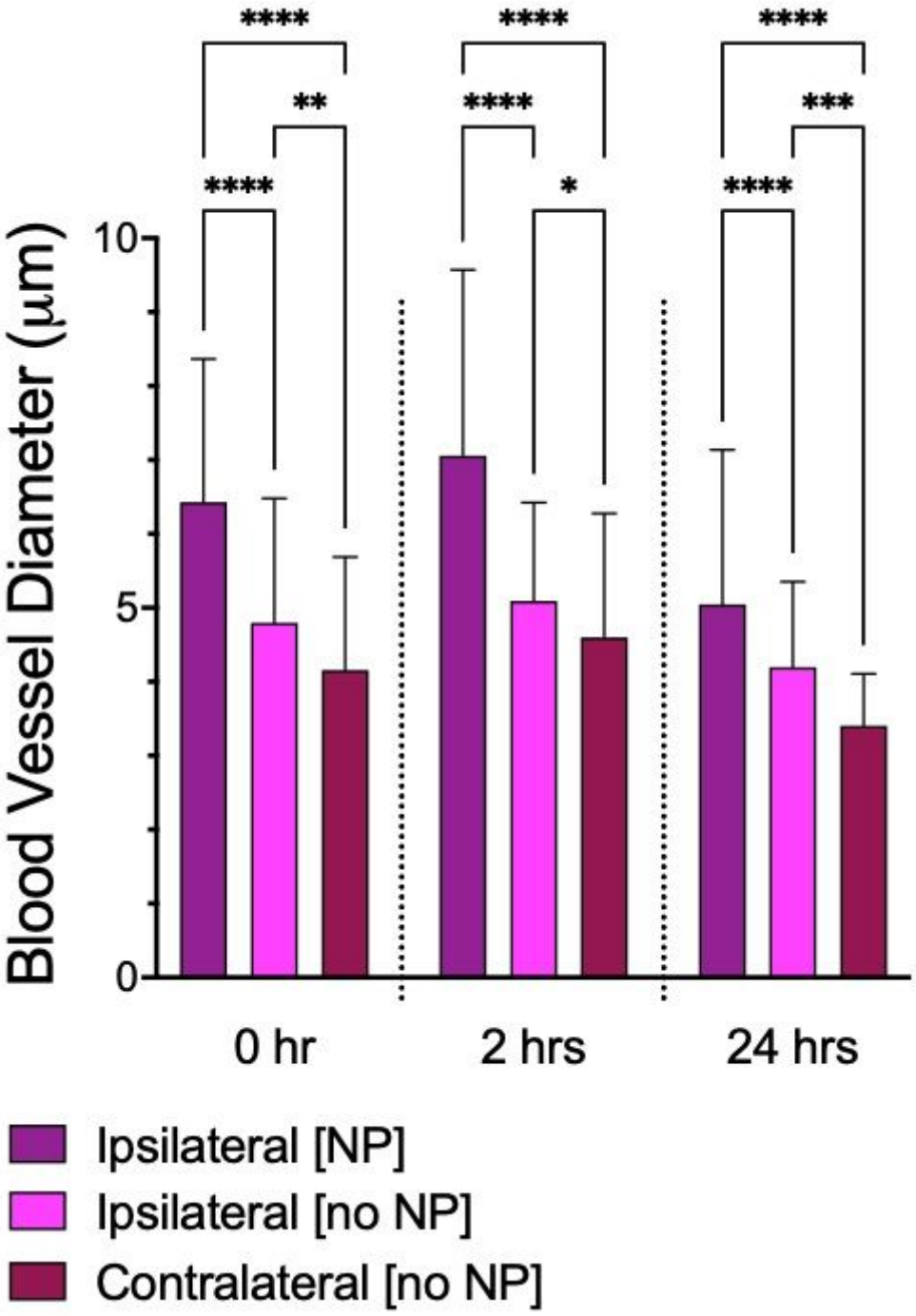

Figure 4

There were significant differences in vessel properties for capillaries that did or did not contain FNPs (Figure 4).

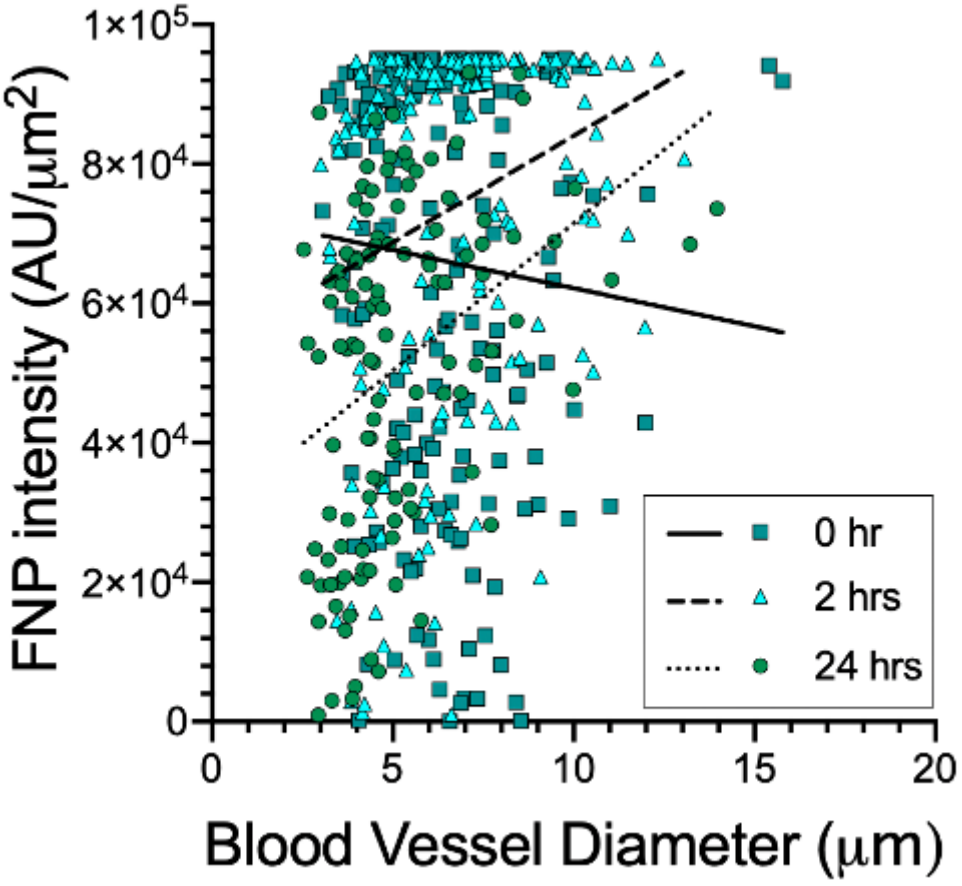

Figure 5

In contrast, when FNPs were administered 2 or 24 hours after resection, larger vessels contained brighter FNP clusters with a higher ROI intensity (Figure 5).